Sliding modes and Lyapunov functions for differential inclusions by linear programming ⋆

Sigurdur Hafstein[0000−0003−0073−2765]

Science Institute, University of Iceland, Dunhagi 5, 107 Reykjavík, Iceland
shafstein@hi.is

Abstract. Recently the concept of essential neighbours of simplices was introduced for switched systems and differential inclusions with triangulated state spaces. It was used to design an algorithm that was able to compute Lyapunov functions for such systems with a strongly asymptotically stable equilibrium, of which the Filippov regularization does not have a strongly asymptotically stable equilibrium. Here we advance this algorithm further and show that the methodology can additionally be used to localize the sliding modes is differential inclusions. Using this localization we can remove constraints from a linear programming problem, whose feasible solutions parameterize Lyapunov functions for the system. We demonstrate the efficacy of our new approach for three systems from the literature.

Keywords: Lyapunov function, Switched systems, Differential inclusions, Sliding modes, Numerical algorithm,

1 INTRODUCTION

Switched systems and differential inclusions, in particular Filippov regularizations/convexifications [21], have received much attention in engineering and the applied sciences because they allow for the efficient modelling of complex phenomena, cf. e.g. [5,43,6,8,9,28] for some relevant references on differential inclusions and [13,1,16,40,49,44,2,47] for switched systems.

Because there can be and often are multiple trajectories emerging from a given initial value, one must differ between weakly- and strongly asymptotically stable equilibrium points. That is, does at least one solution trajectory for every initial value in a neighbourhood of an equilibrium converge to it (weak stability) or does every trajectory for every such initial value converge to it (strong stability). The latter concept can be characterized using Lyapunov functions [15] and the former using so-called control Lyapunov functions [45,46]. Both must be studied in the framework of nonsmooth analysis [14].

In [35] the author introduced the concept of *essential neighbours* of simplices for state switched systems/differential inclusions, of which the state space has

⋆ This research was supported by the Icelandic Research Fund (Rannís) grant number 163074-052, Complete Lyapunov functions: Efficient numerical computation.

been triangulated, and how non-essential neighbours can be rigorously identified and removed algorithmically. This was then used to advance the algorithm developed in [31,8,9,10] to compute Continuous and Piecewise Affine (CPA) Lyapunov functions using linear programming (LP). In this paper we improve the results from [35] still further and show how the essential neighbours can be used to identify and localize sliding modes. Further, we show how this information can be used to generate improved LP problems with fewer constraints for the computation of CPA Lyapunov functions.

The paper is structured as follows: In Section 2 we describe and discuss switched systems and differential inclusions. In Section 3 we recall various definitions and results about triangulations and CPA functions. In particular we define the systems we tackle with our algorithms in Section 3.2. In Section 4 we present our algorithms, **Algorithm SM** that localizes the sliding modes and **Algorithm CPA** that computes a CPA Lyapunov function for the system in question. In Section 5 we compute the sliding modes and CPA Lyapunov functions for three systems from the literature, before we conclude the paper in Section 6.

2 SWITCHED SYSTEMS AND DIFFERENTIAL INCLUSIONS

We consider switched systems that are generated by a finite set of ordinary differential equations (ODEs),

$$\dot{\mathbf{x}} = \mathbf{f}_\alpha(\mathbf{x}), \quad \alpha : [0,\infty) \to \mathcal{A}, \tag{1}$$

where $\mathcal{A}$ is a finite index set and for each $a \in \mathcal{A}$ the domain of the locally Lipschitz vector field $\mathbf{f}_a : \mathcal{D}(\mathbf{f}_a) \to \mathbb{R}^n$ is $\mathcal{D}(\mathbf{f}_a) \subset \mathbb{R}^n$. The switching is realized through the mapping $\alpha : [0,\infty) \to \mathcal{A}$, called switching signal. Solution trajectories of the system are continuous paths obtained by gluing together trajectory pieces of the individual systems $\dot{\mathbf{x}} = \mathbf{f}_a(\mathbf{x})$. That is, for an initial value $\boldsymbol{\xi} \in \mathcal{D} := \bigcup_{a\in\mathcal{A}} \mathcal{D}(\mathbf{f}_a)$ and a switching signal α we say that $t \mapsto \boldsymbol{\phi}_\alpha(t,\boldsymbol{\xi})$ is a solution to (1) with initial value $\boldsymbol{\xi}$ if it is absolutely continuous,

$$\phi_\alpha(0,\boldsymbol{\xi}) = \boldsymbol{\xi} \quad \text{and} \quad \frac{d}{dt}\boldsymbol{\phi}_\alpha(t,\boldsymbol{\xi}) = \mathbf{f}_{\alpha(t)}(\boldsymbol{\phi}_\alpha(t,\boldsymbol{\xi})) \;\; \text{a.s.} \tag{2}$$

Recall that 'a.s.' stands for 'almost surely', i.e. the set of those t where the condition is not fulfilled in contained in a set of measure zero. Note that not any function $\alpha : [0,\infty) \to \mathcal{A}$ can serve as a switching signal. Common restrictions are e.g. that α is right-continuous when $\mathcal{A}$ is equipped with the discrete topology and that there are only finitely many points of discontinuity on any bounded interval.

As usual for differential equations we assume $t \mapsto \boldsymbol{\phi}_\alpha(t,\boldsymbol{\xi})$ is defined on a maximum half-open interval $I_{\alpha,\boldsymbol{\xi}} = [0,c)$, $c > 0$, i.e. it cannot be extended to fulfill the solution conditions on a larger interval.

A novel complication in comparison to ODEs is that solutions can get stuck due to the switching as illustrated in the following simple example.

Example 1. Consider the switched system (1) with $\mathcal{A} := \{1,2\}$, $f_1 : (-\infty, 0] \to \mathbb{R}$, $f_1(x) = 1$, and $f_2 : [0,\infty) \to \mathbb{R}$, $f_2(x) = -1$. For an initial value $\xi < 0$ we have the solution $\phi_\alpha(t,\xi) = \xi + t$, where necessarily $\alpha(t) = 1$ for $0 \leq t < -\xi$. A different switching α with values in $\{1,2\}$ is not possible. At time $t = -\xi$ there is a problem because f_1 is pushing the trajectory into $[0,\infty)$ and if $\phi_\alpha(t,\xi) > 0$ we must set $\alpha(t) = 2$, i.e. switch to f_2. However, f_2 will immediately push the solution back to $(-\infty, 0)$, where f_2 is not defined. Thus the maximum interval for the solution is $[0, -\xi)$. Solution trajectories of ODEs always reach the boundary of their domain and this phenomena in switched systems is highly undesirable. □

A common way to deal with the problem in Example 1 is to use the Filippov regularization and consider the differential inclusion

$$\dot{\mathbf{x}} \in \mathbf{F}(\mathbf{x}) := \operatorname{co}\{\mathbf{f}_a(\mathbf{x}) : \mathbf{x} \in \mathcal{D}(\mathbf{f}_a)\}, \tag{3}$$

where

$$\operatorname{co} C := \left\{ \sum_{i=0}^{k} \lambda_i \mathbf{x}_i : k \in \mathbb{N}_0,\ \mathbf{x}_i \in C,\ \lambda_i \in [0,1],\ \sum_{i=0}^{k} \lambda_i = 1 \right\}$$

denotes the convex hull of the set $C \subset \mathbb{R}^n$. Solution trajectories to (3) are defined similarly to solutions in the sense of Carathéodory, cf. e.g. [48, §10]. A solution trajectory $t \mapsto \boldsymbol{\phi}(t,\boldsymbol{\xi})$ to (3) with initial value $\boldsymbol{\xi}$ is an absolutely continuous function fulfilling

$$\boldsymbol{\phi}(0,\boldsymbol{\xi}) = \boldsymbol{\xi} \quad \text{and} \quad \frac{d}{dt}\boldsymbol{\phi}(t,\boldsymbol{\xi}) \in \mathbf{F}(\boldsymbol{\phi}(t,\boldsymbol{\xi})) \ \text{ a.s.} \tag{4}$$

Now there are no problems extending the solution from Example 1 to $[0,\infty)$. Just note that

$$\mathbf{F}(x) = \begin{cases} \{1\}, & \text{if } x < 0, \\ [-1,1], & \text{if } x = 0, \\ \{-1\}, & \text{if } x > 0. \end{cases}$$

and $\phi(t,\xi) = t + \xi$ for $0 \leq t < -\xi$ and $\phi(t,\xi) = 0$ for $t \geq -\xi$ is a solution defined on $[0,\infty)$, where we are using the right-hand side $\mathbf{F}(\phi(t,\xi)) = \{f_1(t+\xi)\} = \{1\}$ for $0 \leq t < -\xi$ and

$$\left\{ \frac{1}{2} f_1(\phi(t,\xi)) + \frac{1}{2} f_2(\phi(t,\xi)) \right\} = \{0\} \subset \mathbf{F}(\phi(t,\xi))$$

for $t \geq -\xi$.

An additional advantage of using differential inclusions rather than switched systems, is that there exists a mature theory for closed convex valued, i.e. $\mathbf{F}(\mathbf{x}) = \overline{\operatorname{co}\mathbf{F}(\mathbf{x})}$ for all $\mathbf{x} \in \mathcal{D}$, and upper semicontinuous $\mathbf{F}$, cf. e.g. [6,17]. The mapping

$\mathbf{F} : \mathcal{D} \to \mathfrak{P}(\mathbb{R}^n)$, $\mathcal{D} \subset \mathbb{R}^n$ and where $\mathfrak{P}(\mathbb{R}^n)$ denotes the power-set of $\mathbb{R}^n$ (set of all subsets), is said to be upper semicontinuous if

$$\forall \mathbf{x} \in \mathcal{D}, \forall \epsilon > 0, \exists \delta > 0 : \forall \mathbf{y} \in (\mathbf{x} + \delta B_1) \cap \mathcal{D}, \quad \mathbf{F}(\mathbf{y}) \subset \mathbf{F}(\mathbf{x}) + \epsilon B_1,$$

where B_1 is the open unit ball in $\mathbb{R}^n$. A mapping $\mathbf{F} : \mathcal{D} \to \mathfrak{P}(\mathbb{R}^n)$ is often written as $\mathbf{F} : \mathcal{D} \rightrightarrows \mathbb{R}^n$ and is referred to as multivalued mapping. There are many other characterizations of "upper semicontinuous", e.g. $\mathbf{F}^{-1}(A)$ closed in $\mathcal{D}$ for closed $A \subset \mathbb{R}^n$. Further, the strong asymptotic stability of an equilibrium has been shown to be equivalent to the existence of a smooth, i.e. C^∞, Lyapunov function [15].

However, in some cases the results from the Filippov regularization of a switched systems and the corresponding differential inclusion does not deliver the desired results when studying strong asymptotic stability, as shown in the next example.

Example 2. We consider Artstein's circles [4], also discussed in detail in [35]. We set $\mathcal{A} := \{+, -\}$, $\mathcal{D}(\mathbf{f}_+) = [0, \infty) \times \mathbb{R}$, and $\mathcal{D}(\mathbf{f}_-) = (-\infty, 0] \times \mathbb{R}$ for

$$\mathbf{f}_+(x, y) = \begin{pmatrix} -x^2 + y^2 \\ -2xy \end{pmatrix} \quad \text{and} \quad \mathbf{f}_-(x, y) = -\mathbf{f}_+(x, y) = \begin{pmatrix} x^2 - y^2 \\ 2xy \end{pmatrix}. \tag{5}$$

See Figure 1 taken from [35] for its solution trajectories.

Now consider the Filippov regularization of the switched system, i.e. the system

$$\frac{d}{dt}\begin{pmatrix} x \\ y \end{pmatrix} \in \mathbf{F}(x, y) := \mathrm{co}\{\mathbf{f}_+(x, y), \mathbf{f}_-(x, y)\} := \begin{cases} \{\mathbf{f}_+(x, y)\} & \text{if } x > 0 \\ \{\mathbf{f}_-(x, y)\} & \text{if } x < 0 \\ [-y^2, y^2] \times \{0\}, & \text{if } x = 0. \end{cases} \tag{6}$$

For this differential inclusion the origin is not strongly asymptotically stable, because $0 \in [-y^2, y^2]$ for all $y \in \mathbb{R}$ and thus, for the initial value $\boldsymbol{\xi} = (0, y_0)$, we have the solution trajectory $\boldsymbol{\phi}(t, \boldsymbol{\xi}) = (0, y_0)$ for all $t \in [0, \infty)$, corresponding to $\mathbf{0} \in \mathrm{co}\{\mathbf{f}_+(0, y_0), \mathbf{f}_-(0, y_0)\}$, in addition to the solution trajectories traversing the circle arcs to the left or to the right. Thus the origin is a weakly asymptotically stable equilibrium, but not strongly asymptotically stable, for the Filippov regularization.

However, if we set $\mathbf{F}(x, y)$ to $\{\mathbf{f}_+(x, y), \mathbf{f}_-(x, y)\}$ when $x = 0$, i.e. not the convex hull, or by simply restricting e.g. $\mathbf{f}_+(x, y)$ to $(0, \infty) \times \mathbb{R}$ instead of $[0, \infty) \times \mathbb{R}$, then the origin is strongly asymptotically stable, and this seems more natural because solutions being stuck at $(0, y)$, $y \neq 0$, for system (6) is not robust to infinitesimal perturbations in the system state.

The deficit of not using the Filippov regularization is that then the standard mature theory for differential inclusions with closed convex valued and upper semicontinuous $\mathbf{F} : \mathcal{D} \rightrightarrows \mathbb{R}^n$ does not apply.

Note that $\{\mathbf{f}_+(0, y), \mathbf{f}_-(0, y)\}$ is not convex for $y \neq 0$ and

$$\widetilde{\mathbf{F}}(x, y) := \begin{cases} \{\mathbf{f}_+(x, y)\} \text{ if } x > 0 \\ \{\mathbf{f}_-(x, y)\} \text{ if } x \leq 0 \end{cases}$$

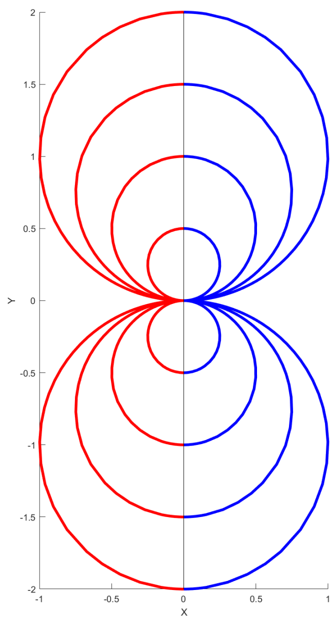

Fig. 1. Trajectories of the switched system (1) with the right-hand side given by (5) (Artstein's circles). For $x > 0$ the system traverses the blue circle arcs to zero and for $x < 0$ the systems traverses the red circle arcs to zero.

is not upper semicontinuous; for $0 < \varepsilon < y^2/2$ and small $x > 0$ we have

$$\widetilde{\mathbf{F}}(x, y) \not\subset \widetilde{\mathbf{F}}(0, y) + \varepsilon B_1 \subset (-\varepsilon - y^2, -y^2 + \varepsilon) \times (-\varepsilon, \varepsilon)$$

because

$$\overline{\bigcap_{x>0} \widetilde{\mathbf{F}}(x, y)} = \{(y^2, 0)\} \quad \text{and} \quad (-\varepsilon - y^2, -y^2 + \varepsilon) \subset (-3y^2/2, -y^2/2).$$

Nevertheless, it seems harmless to use $\widetilde{\mathbf{F}}$ instead of $\mathbf{F}$ considering that no system trajectory can reach the set $\{(0, y) : y \neq 0\}$ because it is repelling. A point in this set is only on a solution trajectory as its initial value. This point was taken in [35]. □

In the following we will study the differential inclusions

$$\dot{\mathbf{x}} \in \mathbf{F}(\mathbf{x}), \quad \mathbf{F}(\mathbf{x}) \supset \{\mathbf{f}_a(\mathbf{x}) : \mathbf{x} \in \mathcal{D}(\mathbf{f}_a)\}, \tag{7}$$

related to the switched system (1), i.e. $\mathcal{A}$ is a finite index set and for each $a \in \mathcal{A}$ the domain of the locally Lipschitz vector field $\mathbf{f}_a : \mathcal{D}(\mathbf{f}_a) \to \mathbb{R}^n$ is $\mathcal{D}(\mathbf{f}_a) \subset \mathbb{R}^n$. Further we assume that the $\mathcal{D}(\mathbf{f}_a)$ are n-dimensional polytopes, $\mathcal{D}(\mathbf{f}_a)^\circ \cap \mathcal{D}(\mathbf{f}_b)^\circ = \emptyset$ if $a \neq b$, and $\mathcal{D}(\mathbf{f}_a) \cap \mathcal{D}(\mathbf{f}_b)$ is either empty or a k-dimensional polytope, $0 \le k < n$. A solution to (7) with initial value $\boldsymbol{\xi} \in \mathcal{D} := \bigcup_{a\in\mathcal{A}} \mathcal{D}(\mathbf{f}_a)$ is an absolutely continuous functions $t \mapsto \boldsymbol{\phi}(t,\boldsymbol{\xi})$ fulfilling $\boldsymbol{\phi}(0,\boldsymbol{\xi}) = \boldsymbol{\xi}$ and

$$\frac{d}{dt}\boldsymbol{\phi}(t,\boldsymbol{\xi}) \in \mathbf{F}(\boldsymbol{\phi}(t,\boldsymbol{\xi})) \ \text{ a.s. for } t \in J = [0,c),\ c > 0.$$

For the system (7) there are three essentially different types of how two different vector fields $\mathbf{f}_b$ and $\mathbf{f}_w$, $b, w \in \mathcal{A}$, can meet at a boundary. These are shown and discussed in Figure 2.

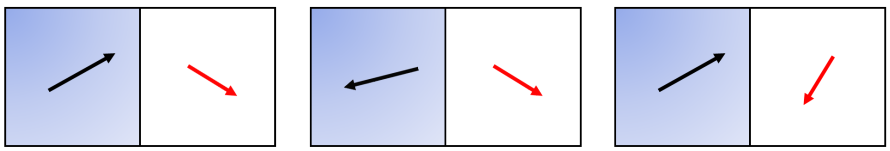

Fig. 2. The three cases of a boundary between two systems, $\dot{\mathbf{x}} = \mathbf{f}_b(\mathbf{x})$ on the left (blue) where the black arrow indicates the vector $\mathbf{f}_b(\mathbf{x})$ and $\dot{\mathbf{x}} = \mathbf{f}_w(\mathbf{x})$ on the right (white) where the red arrow indicates the vector $\mathbf{f}_w(\mathbf{x})$.
Case 1: (left) The black arrow $\mathbf{f}_b(\mathbf{x})$ points towards the boundary and the red arrow $\mathbf{f}_w(\mathbf{x})$ away from it. Thus solutions pass through the boundary.
Case 2: (middle) The black arrow $\mathbf{f}_b(\mathbf{x})$ and the red arrow $\mathbf{f}_w(\mathbf{x})$ point away from the boundary. A solution trajectory can start at the boundary, but otherwise cannot reach it.
Case 3: (right) The black arrow $\mathbf{f}_b(\mathbf{x})$ and the red arrow $\mathbf{f}_w(\mathbf{x})$ point towards the boundary. Thus we have a sliding mode at the boundary.

Let us discuss system (7) in relation to Figure 2. In general, one can set $\mathbf{F}(\mathbf{x}) = \text{co}\{\mathbf{f}_a(\mathbf{x}) : \mathbf{x} \in \mathcal{D}(\mathbf{f}_a)\}$ in system (7), which is the Filippov regularization, and study the stability of an equilibrium assumed to be at the origin using Lyapunov functions. Note that $\mathbf{F}(\mathbf{x}) = \{\mathbf{f}_a(\mathbf{x})\}$ for an $a \in \mathcal{A}$ except in some $\mathcal{D}(\mathbf{f}_b) \cap \mathcal{D}(\mathbf{f}_w)$, which are k-dimensional polytopes, $0 \le k < n$. In [31,8,9,10] an algorithm was developed to compute CPA Lyapunov functions using LP for such systems. However, as we have seen in Example 2 this can be unnecessary restrictive and in [35] it was shown that one can replace $\mathbf{F}(\mathbf{x}) = \text{co}\{\mathbf{f}_a(\mathbf{x}) : \mathbf{x} \in \mathcal{D}(\mathbf{f}_a)\}$ by $\mathbf{F}(\mathbf{x}) = \{\mathbf{f}_a(\mathbf{x}) : \mathbf{x} \in \mathcal{D}(\mathbf{f}_a)\}$ at boundaries of type **Case 2**. This led to LP problems with fewer constraints and one can for example compute a CPA Lyapunov function for Artstein's circles in Example 2. Note that this is not possible with the approaches in [31,8,9,10] because the origin is not strongly asymptotically stable for the Filippov regularization. This is discussed in detail in [35].

For our discussion the gradient of the CPA Lyapunov function to be computed can be assumed to be a constant vector ∇V_b in the blue area and a constant vector ∇V_w in the white area. One definitely has to demand that $\nabla V_b \bullet \mathbf{f}_b(\mathbf{x}) < 0$ in the blue area and $\nabla V_w \bullet \mathbf{f}_w(\mathbf{x}) < 0$ in the white area, if V is to be decreasing along solution trajectories. In [8,9,10] one added the decrease conditions

$$\nabla V_b \bullet \mathbf{f}_w(\mathbf{x}) < 0 \quad \text{and} \quad \nabla V_w \bullet \mathbf{f}_b(\mathbf{x}) < 0 \quad \text{at the boundary.} \tag{8}$$

A feasible solution to the resulting LP problem delivers a CPA Lyapunov functions for the system (7) with $\mathbf{F}(\mathbf{x}) = \text{co}\{\mathbf{f}_a(\mathbf{x}) : \mathbf{x} \in \mathcal{D}(\mathbf{f}_a)\}$, i.e. the Filippov regularization.

In [35] it was shown that one can drop the constraints (8) at boundaries of type **Case 2** and a feasible solution to the resulting LP problem, with fewer constraints, delivers a CPA Lyapunov functions for the system (7) with $\mathbf{F}(\mathbf{x}) = \{\mathbf{f}_a(\mathbf{x}) : \mathbf{x} \in \mathcal{D}(\mathbf{f}_a)\}$ with boundaries of type **Case 2** and $\mathbf{F}(\mathbf{x}) = \text{co}\{\mathbf{f}_a(\mathbf{x}) : \mathbf{x} \in \mathcal{D}(\mathbf{f}_a)\}$ at boundaries of **Case 1** and **Case 3**.

A novel observation in this paper is that one can also drop the constraints (8) at boundaries of type **Case 1**. The reason for this is that when the solution moves from the blue area to the white one, this happens at one time instance which has measure zero. If neither $\mathbf{f}_b(\mathbf{x})$ nor $\mathbf{f}_w(\mathbf{x})$ is tangential to the boundary at the boundary this is obvious, but also in the case that one or both are tangential at some points one can drop the condition because by [35, Lemma 2.1] $\nabla V_b \bullet \mathbf{t} = \nabla V_w \bullet \mathbf{t}$ for any vector $\mathbf{t}$ tangent to the boundary; just note that the trajectory is being held at the boundary by either $\mathbf{f}_b(\mathbf{x})$ or $\mathbf{f}_w(\mathbf{x})$, not a nontrivial convex combination of both. Recall that stability in the Lyapunov theory is proved by considering the integral $\int_0^\infty DV(\boldsymbol{\phi}(t,\boldsymbol{\xi}))dt$, where DV is the derivative of the Lyapunov function V along solution trajectories (in some appropriate sense), for CPA Lyapunov functions cf. [42, Thm. 1.16], and the value of this integral is invariant to altering $t \mapsto DV(\boldsymbol{\phi}(t,\boldsymbol{\xi}))$ on a set of measure zero.

We thus only need to apply constraints (8) at boundaries of type **Case 3**, where the solution trajectory of the system is indeed steered by a nontrivial convex combination of the vector fields $\mathbf{f}_b(\mathbf{x})$ and $\mathbf{f}_w(\mathbf{x})$, see Figure 3. Such a boundary is called a *sliding mode* or a *sliding surface* and has numerous applications in control, cf. e.g. [20,50,11] for a practical applications.

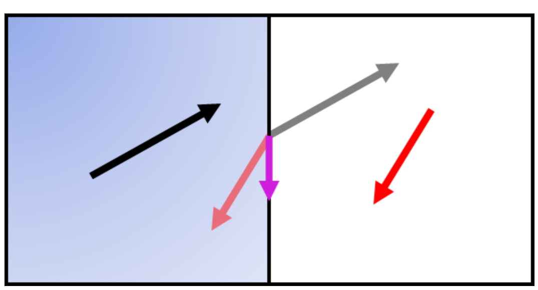

Fig. 3. The sliding mode from Figure 2 **Case 3**. The vector $\lambda_1\mathbf{f}_b(\mathbf{x}) + \lambda_2\mathbf{f}_w(\mathbf{x})$ (magenta) is a nontrivial convex combination of the vectors $\mathbf{f}_b(\mathbf{x})$ (black) and $\mathbf{f}_w(\mathbf{x})$ (red) that is tangent to the boundary. The solution to the system can and must move along the boundary in the direction of this vector.

3 TRIANGULATIONS AND CPA FUNCTIONS

The CPA method was originally an algorithm to compute Lyapunov functions for ODE systems [41,29,30] and in a series of papers [22,23,26] it was proved that it can compute a Lyapunov function for any such system with an exponentially stable equilibrium. Its efficient implementation has been studied in [32,12,33,34] and it has been extended to various other system types, e.g. discrete time systems [24,39], ISS systems [38,39], and finite time systems [37]. In particular, it was extended to arbitrary switched systems in [31] and to differential inclusions with strongly asymptotically stable equilibrium in [8,9]. In [10] a corresponding algorithm was developed for the computation of control CPA Lyapunov functions for weakly asymptotically stable differential inclusions, see also [7] for a different approach including semiconcavity condition into the formulation of the optimization problem.

A CPA Lyapunov function is a Lyapunov function that is continuous and piecewise affine on every simplex of a triangulation. Thus, to define a CPA Lyapunov function V, first a triangulation $\mathcal{T}$ of its domain $\mathcal{D}_\mathcal{T} \subset \mathbb{R}^n$ must be fixed. The triangulation must be shape-regular, i.e. any two different simplices must be disjoint or intersect in a common face. The continuous and piecewise affine function V is then defined by assigning it values at the vertices of the simplices of $\mathcal{T}$ and linearly interpolating these values over the simplices. The resulting function is affine on each simplex $S_\nu \in \mathcal{T}$ and has the formula $V(\mathbf{x}) = \nabla V_\nu \bullet \mathbf{x} + a_\nu$ on S_ν, where $\nabla V_\nu \in \mathbb{R}^n$ and $a_\nu \in \mathbb{R}$. In particular, its gradient $\nabla V(\mathbf{x})$ is a well defined constant vector ∇V_ν in the interior S_ν°. At the boundaries, where two or more simplices intersect, the function V is not differentiable and its gradient is cannot defined in the classical sense. We recall numerous definitions and results from [35] before we state our algorithms.

3.1 TRIANGULATIONS

Let $C = \{\mathbf{x}_0, \mathbf{x}_1, \ldots, \mathbf{x}_n\} \subset \mathbb{R}^n$ be a set of affinely independent vectors, i.e. the augmented vectors $(\mathbf{x}_0, 1), (\mathbf{x}_1, 1), \ldots, (\mathbf{x}_n, 1) \in \mathbb{R}^{n+1}$ are linearly independent. The convex hull of the vectors in C, i.e. the set

$$S = \operatorname{co} C = \left\{ \sum_{k=0}^{n} \lambda_k \mathbf{x}_k \,:\, \mathbf{x}_k \in C, \quad \lambda_k \in [0,1], \quad \sum_{k=0}^{n} \lambda_k = 1 \right\},$$

is called a proper n-simplex. The faces of the simplex S are the sets

$$\left\{ \sum_{j=0}^{m} \lambda_{k_j} \mathbf{x}_{k_j} \,:\, \mathbf{x}_{k_j} \in C, \quad \lambda_{k_j} \in [0,1], \quad \sum_{j=0}^{m} \lambda_{k_j} = 1 \right\},$$

where $0 \le m < n$ and $0 \le k_0 < k_1 < \ldots < k_m \le n$. Hence for every subset $\emptyset \neq C' \subsetneq C$ we get a face of the simplex S, namely the set $\operatorname{co} C'$.

Let $\{S_\nu\}_{\nu \in T} = \mathcal{T}$, T an index set, be a set of proper n-simplices in $\mathbb{R}^n$, such that different simplices $S_\nu, S_\mu \in \mathcal{T}$ intersect in a common face or not at all and such that for $\mathcal{D}_\mathcal{T} = \bigcup_{\nu\in T} S_\nu$ the set $\mathcal{D}_\mathcal{T}^\circ$ is a simply connected neighborhood of the origin. The set $\mathcal{T}$ is referred to as a *shape-regular triangulation*. We refer to the set

$$\mathcal{V}_\mathcal{T} := \{\mathbf{x}_i \,:\, \mathbf{x}_i \text{ is a vertex of a simplex } S_\nu \in \mathcal{T}\}$$

as the *vertex set* of the triangulation $\mathcal{T}$.

For each $S_\nu \in \mathcal{T}$, $\nu \in T$, define $C_\nu := \{\mathbf{x}_0^\nu, \mathbf{x}_1^\nu, \ldots, \mathbf{x}_n^\nu\}$ to be the set of its vertices. The shape-regularity can be expressed as: from $S_\nu, S_\mu \in \mathcal{T}$ follows $S_\nu \cap S_\mu = \mathrm{co}(C_\nu \cap C_\mu)$.

3.2 THE SYSTEM CONSIDERED

In the rest of the paper we will consider the differential inclusion (7), i.e.

$$\dot{\mathbf{x}} \in \mathbf{F}(\mathbf{x}), \quad \mathbf{F}(\mathbf{x}) \supset \{\mathbf{f}_a(\mathbf{x}) \,:\, \mathbf{x} \in \mathcal{D}(\mathbf{f}_a)\},$$

that is adapted to the shape-regular triangulation $\mathcal{T}$. In more detail:

Let a shape-regular triangulation $\mathcal{T} = \{S_\nu\}_{\nu\in T}$ in $\mathbb{R}^n$ and a finite number of C^2 vector fields $\mathbf{f}_a : \mathcal{D}(\mathbf{f}_a) \to \mathbb{R}^n$, $a \in \mathcal{A}$ an index set, be given. Assume that for every $a \in \mathcal{A}$ the domain $\mathcal{D}(\mathbf{f}_a) \subset \mathbb{R}^n$ of $\mathbf{f}_a$ is the (nonempty) union of some of the simplices in $\mathcal{T}$, i.e.

$$\emptyset \neq \mathcal{D}(\mathbf{f}_a) = S_{\nu_1} \cup S_{\nu_2} \cup \cdots \cup S_{\nu_k}, \quad \text{where } \nu_1, \nu_2, \ldots, \nu_k \in T$$

and that $\mathcal{D}(\mathbf{f}_a)^\circ \cap \mathcal{D}(\mathbf{f}_b)^\circ = \emptyset$ if $a \neq b$.

Define for every $\nu \in T$ the set $\mathcal{A}_\nu := \{a \in \mathcal{A} \,:\, S_\nu \subset \mathcal{D}(\mathbf{f}_a)\}$ and assume that $\mathcal{A}_\nu \neq \emptyset$ for all $\nu \in T$. Hence, every simplex $S_\nu \in \mathcal{T}$ is entirely in the domain of exactly one vector field $\mathbf{f}_a$.

3.3 ESTIMATES

The following estimates are of essential importance for the CPA algorithm, because they allow us to check certain inequalities at the vertices $\mathcal{V}_\mathcal{T}$ of the simplices in $\mathcal{T}$ to gain estimates on the entire domain $\mathcal{D}_\mathcal{T}$.

For a set $C = \{\mathbf{x}_0, \mathbf{x}_1, \ldots, \mathbf{x}_k\}$ of affinely independent vectors in $\mathbb{R}^n$ and a C^2 vector field $\mathbf{f}_a$ defined on $\mathrm{co}\, C$ with components $(f_1^a, f_2^a, \ldots, f_n^a) = \mathbf{f}_a$ define a constant $B_{C,r,s}^a$ such that

$$B_{C,r,s}^a \geq \max_{\substack{\mathbf{x}\in \mathrm{co}\, C \\ m=1,2,\ldots,n}} \left| \frac{\partial^2 f_m^a}{\partial x_r \partial x_s}(\mathbf{x}) \right|. \tag{9}$$

Further, for each (vertex) $\mathbf{y} \in C$ define

$$C_{\mathbf{y},s}^{\max} := \max_{j=0,1,\ldots,k} |\mathbf{e}_s \bullet (\mathbf{x}_j - \mathbf{y})|$$

and set

$$E_{C,\mathbf{x}_i}^{a,\mathbf{y}} := \frac{1}{2} \sum_{r,s=1}^{n} B_{C,r,s}^a |\mathbf{e}_r \bullet (\mathbf{x}_i - \mathbf{y})| (C_{\mathbf{y},s}^{\max} + |\mathbf{e}_s \bullet (\mathbf{x}_i - \mathbf{y})|), \tag{10}$$

for $i = 0, 1, \ldots, k$. The constants $E^{a,\mathbf{y}}_{C,\mathbf{x}_i}$ are defined such that if $\emptyset \neq C \subset C_\nu$, i.e. $\operatorname{co} C_\nu = S_\nu \in \mathcal{T}$ or $\operatorname{co} C$ is a face of S_ν, we have for a fixed vector $\mathbf{v} \in \mathbb{R}^n$ and a convex function $p : \mathbb{R}^n \to \mathbb{R}$ that

$$\mathbf{v} \bullet \mathbf{f}_a(\mathbf{x}_i) + E^{a,\mathbf{y}}_{C,\mathbf{x}_i} \|\mathbf{v}\|_1 \leq -p(\mathbf{x}_i), \quad i = 0, 1, \ldots, k, \tag{11}$$

implies $\mathbf{v} \bullet \mathbf{f}_a(\mathbf{x}) \leq -p(\mathbf{x})$ for all $\mathbf{x} \in \operatorname{co} C$.

This follows by [42, Lemma 4.16], which states that for a convex combination of the vertices $\mathbf{x} = \sum_{i=0}^{k} \lambda_i \mathbf{x}_i \in \operatorname{co} C$ we have the estimate

$$\left\| \mathbf{f}_a(\mathbf{x}) - \sum_{i=0}^{k} \lambda_i \mathbf{f}_a(\mathbf{x}_i) \right\|_\infty \leq \sum_{i=0}^{k} \lambda_i E^{a,\mathbf{y}}_{C_\nu,\mathbf{x}_i}. \tag{12}$$

Hence, by Hölder's inequality and (11) we have that

$$\begin{aligned}
\mathbf{v} \bullet \mathbf{f}_a(\mathbf{x}) &= \sum_{i=0}^{k} \lambda_i \mathbf{v} \bullet \mathbf{f}_a(\mathbf{x}_i) + \mathbf{v} \bullet \left[\mathbf{f}_a(\mathbf{x}) - \sum_{i=0}^{k} \lambda_i \mathbf{f}_a(\mathbf{x}_i) \right] \\
&\leq \sum_{i=0}^{k} \lambda_i \mathbf{v} \bullet \mathbf{f}_a(\mathbf{x}_i) + \|\mathbf{v}\|_1 \left\| \mathbf{f}_a(\mathbf{x}) - \sum_{i=0}^{k} \lambda_i \mathbf{f}_a(\mathbf{x}_i) \right\|_\infty \\
&\leq \sum_{i=0}^{k} \lambda_i \mathbf{v} \bullet \mathbf{f}_a(\mathbf{x}_i) + \|\mathbf{v}\|_1 \cdot \sum_{i=0}^{k} \lambda_i E^{a,\mathbf{y}}_{C_\nu,\mathbf{x}_i} \\
&= \sum_{i=0}^{k} \lambda_i \left(\mathbf{v} \bullet \mathbf{f}_a(\mathbf{x}_i) + \|\mathbf{v}\|_1 E^{a,\mathbf{y}}_{C_\nu,\mathbf{x}_i} \right) \\
&\leq \sum_{i=0}^{k} \lambda_i \left(-p(\mathbf{x}_i) \right) \leq -p\left(\sum_{i=0}^{k} \lambda_i \mathbf{x}_i \right) = -p(\mathbf{x}).
\end{aligned}$$

For implementing the constraints (11) it is of essential practical importance that the $B^a_{C,r,s}$ are just upper bounds. Further, the vertex $\mathbf{y} \in C$ for $E^{a,\mathbf{y}}_{C,\mathbf{x}_i}$ in (11) is arbitrary, but must be the same for all $i = 0, 1, \ldots, k$. In our application p is a nonnegative function and $\mathbf{f}_a(\mathbf{0}) = \mathbf{0}$. If $\mathbf{0} \in C$ and $B^a_{C,r,s} > 0$, then $\mathbf{y} = \mathbf{0}$ is the only sensible choice because $E^{a,\mathbf{y}}_{C,\mathbf{y}} = 0$. Additionally, if $\mathbf{0} \in \operatorname{co} C$ we must have $\mathbf{0} \in C$ if (11) is to be fulfilled.

ESSENTIAL NEIGHBOURS

For a simplex $S_\nu \in \mathcal{T}$ define the set

$$NS_\nu := \{ S_\mu \in \mathcal{T} : S_\mu \neq S_\nu \text{ and } S_\mu \cap S_\nu \neq \emptyset \}$$

of its neighbouring simplices in $\mathcal{T}$. In [35] the set of the *essential neighbouring simplices* ENS^a_ν, $a \in \mathcal{A}_\nu$, for the simplex S_ν and with respect to the vector field

$\mathbf{f}_a$, was introduced. That is, ENS_ν^a contains the simplices $S_\mu \in NS_\nu$, $a \notin \mathcal{A}_\mu$, with an initial position $\mathbf{x} \in S_\nu$ such that the solution trajectory of $\dot{\mathbf{x}} = \mathbf{f}_a(\mathbf{x})$ moves into the interior of S_μ in an infinitesimal time. In formula, for every $S_\nu \in \mathcal{T}$ and $a \in \mathcal{A}_\nu$ define

$$ENS_\nu^a := \{S_\mu \in NS_\nu \,:\, a \notin \mathcal{A}_\mu \text{ and } \exists \mathbf{x} \in S_\nu, \exists h > 0 \text{ s.t. } \mathbf{x} + (0,h]\mathbf{f}_a(\mathbf{x}) \subset S_\mu^\circ\}.$$

Note that we have made the definition a little more restrictive than in [35], where 'can move into the interior of S_μ in an infinitesimal time' and the condition '$\mathbf{x} + [0,h]\mathbf{f}_a(\mathbf{x}) \subset S_\mu$' were used. Further, we removed all $S_\mu \in NS_\nu$ with $a \in \mathcal{A}_\mu$ from the set ENS_ν^a, which simplifies the definition of our algorithms below.

4 THE ALGORITHMS

We now describe our algorithms that generate linear inequalities to localize the sliding modes, i.e. boundaries of type **Case 3** in Figure 2, and an LP problem of which any feasible solution parameterizes a CPA Lyapunov functions for the differential inclusion in Section 3.2. We refer to the former as **Algorithm SM**, where **SM** hints at the sliding modes we are interested in, and the latter as **Algorithm CPA**, because it constructs an LP problem which parameterizes a CPA Lyapunov function.

4.1 COMPUTING ESSENTIAL NEIGHBOURS

Consider a simplex $S_\nu = \operatorname{co} C_\nu \in \mathcal{T}$, where as before $C_\nu = \{\mathbf{x}_0^\nu, \mathbf{x}_1^\nu, \ldots, \mathbf{x}_n^\nu\}$. Another way to describe the simplex S_ν is to define it as the intersection of $n+1$ half-spaces $\{\mathbf{x} \in \mathbb{R}^n \,:\, \mathbf{n} \bullet (\mathbf{x} - \mathbf{y}) \geq 0\}$, where $\mathbf{n}, \mathbf{y} \in \mathbb{R}^n$, $\mathbf{n} \neq \mathbf{0}$. These half-spaces for S_ν can be constructed as follows using the set C_ν, cf. [33,35].

For $i = 0, 1, \ldots, n$ we construct the half-space $H_{\nu,\mathbf{x}_i^\nu}$ such that $S_\nu \subset H_{\nu,\mathbf{x}_i^\nu}$ and $C_\nu \setminus \{\mathbf{x}_i^\nu\}$ is a subset of the boundary $\partial H_{\nu,\mathbf{x}_i^\nu}$ of $H_{\nu,\mathbf{x}_i^\nu}$ in the following way:

Set $\mathbf{y}_n := \mathbf{x}_i^\nu$ and pick an arbitrary, but fixed vector $\mathbf{y}_0 \in C_\nu \setminus \{\mathbf{x}_i^\nu\}$. Let $\{\mathbf{y}_1, \mathbf{y}_2, \ldots, \mathbf{y}_{n-1}\} = C_\nu \setminus \{\mathbf{y}_0, \mathbf{y}_n\}$ and define the (nonsingular) matrix

$$Y_{\nu,\mathbf{x}_i^\nu} := (\mathbf{y}_1 - \mathbf{y}_0, \mathbf{y}_2 - \mathbf{y}_0, \ldots, \mathbf{y}_n - \mathbf{y}_0)^\top.$$

With $\mathbf{n}_{\nu,\mathbf{x}_i^\nu} = Y_{\nu,\mathbf{x}_i^\nu}^{-1}\mathbf{e}_n$ the desired half-space is given by

$$H_{\nu,\mathbf{x}_i^\nu} := \{\mathbf{x} \in \mathbb{R}^n \,:\, \mathbf{n}_{\nu,\mathbf{x}_i^\nu} \bullet (\mathbf{x} - \mathbf{y}_0) \geq 0\}. \tag{13}$$

To compute algorithmically a tight upper approximation $(ENS_\nu^a)^*$ of ENS_ν^a, i.e.

$$ENS_\nu^a \subset (ENS_\nu^a)^* \subset NS_\nu,$$

we proceed as follows:

Algorithm SM: For each $S_\nu \in \mathcal{T}$ and $a \in \mathcal{A}_\nu$ start with

$$(ENS_\nu^a)^* = \{S_\mu \in NS_\nu \,:\, a \notin \mathcal{A}_\mu\}.$$

Then for every $S_\nu \in \mathcal{T}$ and each $S_\mu \in (ENS^a_\nu)^*$ do the following:

Let $\{\mathbf{z}_1, \mathbf{z}_2, \dots, \mathbf{z}_r\} = C_\nu \cap C_\mu$ and $\{\mathbf{y}_1, \mathbf{y}_2, \dots, \mathbf{y}_s\} = C_\mu \setminus C_\nu$. Associated to the half-spaces $H_{\mu,\mathbf{y}_j}$ are the vectors $\mathbf{n}_{\mu,\mathbf{y}_j}$ computed as above, but now for the simplex S_μ and its vertices $C_\mu \supset \{\mathbf{y}_1, \mathbf{y}_2, \dots, \mathbf{y}_s\}$. If for any $j = 1, 2, \dots, s$ we have

$$0 \geq \mathbf{n}_{\mu,\mathbf{y}_j} \bullet \mathbf{f}_a(\mathbf{z}_i) + E^{a,\mathbf{y}}_{C_\nu \cap C_\mu, \mathbf{z}_i} \|\mathbf{n}_{\mu,\mathbf{y}_j}\|_1 \tag{14}$$

for all $i = 1, 2, \dots, r$, then S_μ cannot fulfill the condition for an essential neighbour and we remove S_μ from $(ENS^a_\nu)^*$. □

Recall that $S_\nu \cap S_\mu = \text{co}(C_\nu \cap C_\mu)$ and define

$$\mathcal{F}_{\text{SM}} := \left\{ C_\nu \cap C_\mu \,:\, S_\nu \in (ENS^a_\mu)^* \;\text{ and }\; S_\mu \in (ENS^a_\nu)^* \right\}. \tag{15}$$

It is not difficult to see that $\bigcup_{F \in \mathcal{F}_{\text{SM}}} \text{co}\, F$ is a superset of all sliding modes of the differential inclusion in Section 3.2, i.e. boundaries of type **Case 3** in Figure 2.

For a visual illustration of the sets $(ENS^a_\nu)^*$ see Figure 4 taken from [35].

4.2 PARAMETERIZING CPA LYAPUNOV FUNCTIONS

The LP problem, of which every feasible solution parameterizes a CPA Lyapunov function for the differential inclusion in Section 3.2, has the variables $V_\mathbf{x}$, $\mathbf{x} \in \mathcal{V}_\mathcal{T}$. For every $\mathbf{x}$ that is a vertex of a simplex in $\mathcal{T}$ the LP problem solver will attempt to assign the value of a CPA Lyapunov function V at $\mathbf{x}$ to the variable $V_\mathbf{x}$. From a feasible solution, where the variables $V_\mathbf{x}$ have been assigned values such that the linear constraints below are fulfilled, we then define a continuous function $V : \mathcal{D}_\mathcal{T} \to \mathbb{R}$ through parameterization and interpolation using these values: for an $\mathbf{x} \in \mathcal{D}_\mathcal{T}$ we can find a simplex $S_\nu = \text{co}\{\mathbf{x}^\nu_0, \mathbf{x}^\nu_1, \dots, \mathbf{x}^\nu_n\}$ such that $\mathbf{x} \in S_\nu$ and $\mathbf{x}$ can be written as a convex combination of the vertices $\mathbf{x}^\nu_i$ in a unique way. We then define V at $\mathbf{x}$ as the same convex combination of the values $V_{\mathbf{x}^\nu_i}$, i.e.

$$V(\mathbf{x}) := \sum_{i=0}^{n} \lambda_i V_{\mathbf{x}^\nu_i} \quad \text{where} \quad \mathbf{x} = \sum_{i=0}^{n} \lambda_i \mathbf{x}^\nu_i.$$

If two different simplices in $\mathcal{T}$ intersect they do so in a common face, hence V is well-defined and continuous. By a slight abuse of notation we both write $V(\mathbf{x}^\nu_i)$ for the variable $V_{\mathbf{x}^\nu_i}$ of the LP problem and the value of the function V at $\mathbf{x}^\nu_i$, since they are the same value anyways.

Algorithm CPA: There are two groups of constrains in the LP problem. The first group is to assert that V has a minimum at the origin:

Linear constraints L1
If $\mathbf{0} \in \mathcal{V}_\mathcal{T}$ one sets $V(\mathbf{0}) = 0$. Then for all $\mathbf{x} \in \mathcal{V}_\mathcal{T}$:

$$V(\mathbf{x}) \geq \|\mathbf{x}\|_2.$$

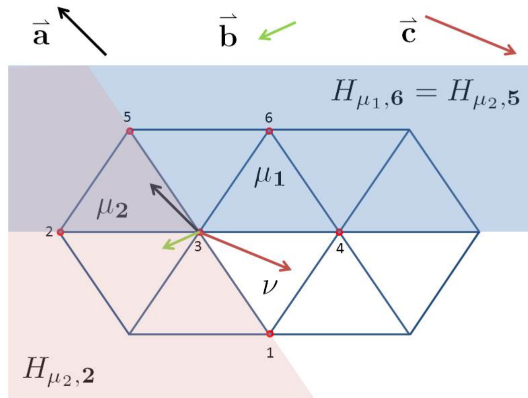

Fig. 4. (extracted from [35]) The simplex S_ν is the convex combination of the $3 = n+1$ vertices $\mathbf{1}, \mathbf{3}, \mathbf{4}$, i.e. $S_\nu = \text{co}\{\mathbf{1}, \mathbf{3}, \mathbf{4}\}$, and $S_{\mu_1} = \text{co}\{\mathbf{3}, \mathbf{4}, \mathbf{6}\}$, and $S_{\mu_2} = \text{co}\{\mathbf{2}, \mathbf{3}, \mathbf{5}\}$. Clearly $\{S_{\mu_1}, S_{\mu_2}\} \subset NS_\nu$. We consider three constant $\mathbf{f}_a(\mathbf{x})$ with $\mathcal{D}(\mathbf{f}_a) = S_\nu$: $\mathbf{f}_1(\mathbf{x}) = \vec{\mathbf{a}}$, $\mathbf{f}_2(\mathbf{x}) = \vec{\mathbf{b}}$, and $\mathbf{f}_3(\mathbf{x}) = \vec{\mathbf{c}}$; depicted by arrows. Since the vector fields are constant the sets ENS_ν^a and $(ENS_\nu^a)^*$ coincide. Now $S_\nu \cap S_{\mu_1} = \text{co}\{\mathbf{3}, \mathbf{4}\}$ and the half-space $H_{\mu_1,\mathbf{6}}$, with $\text{co}\{\mathbf{3}, \mathbf{4}\}$ at its boundary and containing S_{μ_1}, is depicted in blue. We have $S_{\mu_1} \in (ENS_\nu^1)^*$ because $\mathbf{f}_1(\mathbf{x}) = \vec{\mathbf{a}}$ points into $H_{\mu_1,\mathbf{6}}$ for (some) $\mathbf{x} \in \text{co}\{\mathbf{3}, \mathbf{4}\}$ but $S_{\mu_1} \notin (ENS_\nu^a)^*$ for $a = 2, 3$ because $\mathbf{f}_2(\mathbf{x}) = \vec{\mathbf{b}}$ and $\mathbf{f}_3(\mathbf{x}) = \vec{\mathbf{c}}$ do not point into $H_{\mu_1,\mathbf{6}}$ for any $\mathbf{x} \in \text{co}\{\mathbf{3}, \mathbf{4}\}$. Similarly, $S_\nu \cap S_{\mu_2} = \{\mathbf{3}\}$ and the $(n-1)$-faces $\text{co}\{\mathbf{2}, \mathbf{3}\}$ and $\text{co}\{\mathbf{3}, \mathbf{5}\}$ of S_{μ_2} contain $S_\nu \cap S_{\mu_2}$. The half-spaces $H_{\mu_2,\mathbf{5}}$ (blue) and $H_{\mu_2,\mathbf{2}}$ (red) are supersets of S_{μ_2} and with $\text{co}\{\mathbf{2}, \mathbf{3}\}$ and $\text{co}\{\mathbf{3}, \mathbf{5}\}$ at their boundaries, respectively, are depicted. Now $S_{\mu_2} \in (ENS_\nu^1)^*$ because $\mathbf{f}_1(\mathbf{x}) = \mathbf{a}$ points into both $H_{\mu_2,\mathbf{5}}$ (blue) and $H_{\mu_2,\mathbf{2}}$ for $\mathbf{x}$ at the vertex $\mathbf{3}$, but $S_{\mu_2} \notin (ENS_\nu^2)^*$ because $\mathbf{f}_2(\mathbf{x}) = \vec{\mathbf{b}}$ does not point into $H_{\mu_2,\mathbf{5}}$ and $S_{\mu_2} \notin (ENS_\nu^3)^*$ because $\mathbf{f}_2(\mathbf{x}) = \vec{\mathbf{c}}$ does neither point into $H_{\mu_2,\mathbf{5}}$ nor $H_{\mu_2,\mathbf{2}}$.

Another possibility is to relax the condition of strong asymptotic stability of the origin to *practical strong asymptotic stability*. In this case one defines a priori an arbitrary small neighbourhood of the origin $\mathcal{N}$ and does not demand that V is decreasing along solution trajectories in this set. One must then make sure through constraints that

$$\max_{\mathbf{x}\in\partial\mathcal{N}} V(\mathbf{x}) < \min_{\mathbf{x}\in\partial\mathcal{D}_\mathcal{T}} V(\mathbf{x}), \tag{16}$$

because sublevel sets $\mathcal{L}$ of V that are closed in $\mathcal{D}_\mathcal{T}^\circ$ are forward invariant lower bounds on the basin of attraction. This is not difficult to implements and is discussed in detail in e.g. [29,31,9,36]; for example choose $\mathcal{N}$ as the union of a subset of the simplices in $\mathcal{T}$ such that $\max_{\mathbf{x}\in\partial\mathcal{N}} V(\mathbf{x}) = \max_{\mathbf{x}\in\partial\mathcal{N}\cap\mathcal{V}_\mathcal{T}} V(\mathbf{x})$. Then (16) can be implemented as

$$\max_{\mathbf{x}\in\partial\mathcal{N}\cap\mathcal{V}_\mathcal{T}} V(\mathbf{x}) < \min_{\mathbf{x}\in\partial\mathcal{D}_\mathcal{T}\cap\mathcal{V}_\mathcal{T}} V(\mathbf{x}).$$

The implications of such a Lyapunov function are that solutions starting at $\boldsymbol{\xi} \in \mathcal{L}$ enter $\mathcal{N}$ in a finite time and either stay in $\mathcal{N}$ or stay close, i.e.

$$\limsup_{t\to\infty} V(\boldsymbol{\phi}(t,\boldsymbol{\xi})) \le \max_{\mathbf{x}\in\partial\mathcal{N}} V(\mathbf{x})\}.$$

The second group of linear constraints is to assert that V is decreasing along all solution trajectories.

Linear constraints L2
For every $S_\nu \in \mathcal{T}$, we demand for $a \in \mathcal{A}_\nu$ and $i = 0, 1, \ldots, n$ that:

$$\nabla V_\nu \bullet \mathbf{f}_a(\mathbf{x}_i^\nu) + \|\nabla V_\nu\|_1 E^{a;\mathbf{y}}_{C_\nu,\mathbf{x}_i^\nu} \le -\|\mathbf{x}_i^\nu\|_2. \tag{17}$$

For every $F = C_\mu \cap C_\nu = \{\mathbf{x}_0, \mathbf{x}_1, \ldots, \mathbf{x}_k\} \in \mathcal{F}_{\mathrm{SM}}$ and with $a \in \mathcal{A}_\nu$ and $b \in \mathcal{A}_\mu$ we demand for $i = 0, 1, \ldots, k$ that:

$$\nabla V_\mu \bullet \mathbf{f}_a(\mathbf{x}_i) + \|\nabla V_\mu\|_1 E^{a;\mathbf{y}}_{F,\mathbf{x}_i} \le -\|\mathbf{x}_i\|_2 \tag{18}$$

and

$$\nabla V_\nu \bullet \mathbf{f}_b(\mathbf{x}_i) + \|\nabla V_\nu\|_1 E^{a;\mathbf{y}}_{F,\mathbf{x}_i} \le -\|\mathbf{x}_i\|_2 \tag{19}$$

In the case of practical strong asymptotic stability one disregards the constraints (17) for $S_\nu \subset \mathcal{N}$ and the constraints (18) and (19) if either $S_\nu \subset \mathcal{N}$ or $S_\mu \subset \mathcal{N}$. □

Note that the constrains (17), (18), and (19) are all linear in the variables $V(\mathbf{x})$, $\mathbf{x} \in \mathcal{V}_\mathcal{T}$, of the LP problem, cf. e.g. [26, Remarks 9 and 10], and $\|\nabla V_\nu\|_1$ can be modelled through linear constraint using auxiliary variables.

For the following discussion define

$$\mathbf{F}_\mathbf{x} := \{\mathbf{f}_a(\mathbf{x}) \,:\, \mathbf{x} \in \mathcal{D}(\mathbf{f}_a)\} \tag{20}$$

for all $\mathbf{x} \in \mathcal{D}_\mathcal{T}$. A feasible solution to the LP problem constructed by **Algorithm CPA** parameterizes a CPA Lyapunov function V for the differential inclusion from Section 3.2 with

$$\mathbf{F}(\mathbf{x}) := \mathbf{F}_\mathbf{x} \quad \text{if} \quad \mathbf{x} \in \bigcup_{F\in\mathcal{F}_{\mathrm{SM}}} \operatorname{co} F \quad \text{and} \quad \mathbf{F}(\mathbf{x}) := \operatorname{co}\mathbf{F}_\mathbf{x} \quad \text{otherwise}, \tag{21}$$

that fulfills the decrease condition

$$D^+V(\mathbf{x},\mathbf{y}) := \limsup_{h\to 0+} \frac{V(\mathbf{x}+h\mathbf{y}) - V(\mathbf{x})}{h} \le -\|\mathbf{x}\|_2$$

for all $\mathbf{y} \in \mathbf{F}(\mathbf{x})$.

For the fully fledged Clarke subdifferential

$$\partial_{\mathrm{Cl}} V(\mathbf{x}) := \operatorname{co}\{\nabla V_\mu \,:\, \mathbf{x} \in S_\mu\}$$

and the Filippov regularization $\mathbf{F}(\mathbf{x}) = \operatorname{co}\mathbf{F}_{\mathbf{x}}$ of the system in Section 3.2, the set $\partial_{\mathrm{Cl}}V(\mathbf{x}) \bullet \mathbf{F}(\mathbf{x}) \subset \mathbb{R}$ consists of the elements

$$\left(\sum_{\mu\,:\,\mathbf{x}\in S_\mu} \alpha_\mu \nabla V_\mu\right) \bullet \left(\sum_{a\,:\,\mathbf{x}\in\mathcal{D}(\mathbf{f}_a)} \beta_a \mathbf{f}_a(\mathbf{x})\right) = \sum_{\substack{\mu\,:\,\mathbf{x}\in S_\mu \\ a\,:\,\mathbf{x}\in\mathcal{D}(\mathbf{f}_a)}} \alpha_\mu\beta_a \nabla V_\mu \bullet \mathbf{f}_a(\mathbf{x}),$$

for all $\alpha_\mu, \beta_a \geq 0$ fulfilling

$$\sum_{\mu\,:\,\mathbf{x}\in S_\mu} \alpha_\mu = \sum_{a\,:\,\mathbf{x}\in\mathcal{D}(\mathbf{f}_a)} \beta_a = 1.$$

To fulfill $\partial_{\mathrm{Cl}}V(\mathbf{x}) \bullet \mathbf{F}(\mathbf{x}) \leq -\|\mathbf{x}\|_2$ we need

$$\nabla V_\mu \bullet \mathbf{f}_a(\mathbf{x}) \leq -\|\mathbf{x}\|_2 \tag{22}$$

for all μ, a such that $\mathbf{x} \in S_\mu \cap \mathcal{D}(\mathbf{f}_a)$. As we discussed in Section 2 this is unnecessary limiting if we want to prove strong asymptotic stability of the equilibrium at the origin in a more practical sense using formula (21) for $\mathbf{F}$. Our novel algorithms are designed to remove the condition (22) for as many μ, a as possible, but still keep it in place where necessary to secure that solution trajectories of the differential inclusion from Section 3.2 are actually being attracted to the origin. In the next section we demonstrate the efficacy of our approach with three examples from the literature.

5 EXAMPLES

We present three examples of our new algorithms. The methods were implemented in C++ and the LP problems were solved using the Gurobi solver, which is free for academia. Example 5.1 was solved within 2 seconds using a state of the art PC, Examples 5.2 and 5.3 in a split second. The triangulations we used are mapped standard triangulations $\mathcal{T}^{\mathrm{std}}_{N,K}$, with or without a triangle fan at the origin, cf. Figure 5. The implementation and theoretical properties of such triangulations are discussed in detail in [32,25,33,34,3,27], to which the interested reader is referred. The parameters of the computations were fixed through trial-and-error.

5.1 Example 1

The first example is Artstein's circles discussed in Example 2. We set $B^a_{C,r,s} = 2$ uniformly, i.e. for all values of a, C, r, s, cf. (9).

We used the mapped standard triangulation $\mathcal{T}^{\mathrm{std}}_{48,0}$ using the mapping $\mathbf{M}(\mathbf{0}) = \mathbf{0}$ and

$$\mathbf{M}(\mathbf{x}) = 2.5 \cdot 10^{-4} \frac{\|\mathbf{x}\|_\infty^{1.5}}{\|\mathbf{x}\|_2}\mathbf{x} \quad \text{for } \mathbf{x} \neq \mathbf{0}.$$

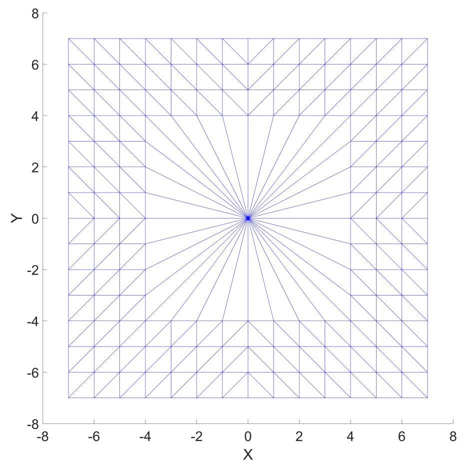

Fig. 5. The standard triangulation $\mathcal{T}^{\text{std}}_{N,K}$ in the plane $\mathbb{R}^2$ with $N = 7$ and $K = 4$. All vertices have integer coordinates, $N \geq K$ fixes the size of the square $[-N, N]^2$ triangulated and $K \geq 0$ fixes the size of the triangle fan at the origin. For $K = 0$ and $K = 1$ there is no triangle fan.

We excluded a small neighbourhood of the origin from the domain of the CPA Lyapunov function to be computed. More exactly we excluded the triangles mapped from $[-4, 4]^2$; i.e. $\mathcal{N} \subset \mathbf{M}((-4, 4)^2) \subset 2 \cdot 10^{-3} B_1$ in the computations. Note that this is necessary, because the existence of a CPA Lyapunov function implies that the origin is exponentially stable, which is not the case for for Artstein's circles as can easily be seen from linearizing $\mathbf{f}_+$ and $\mathbf{f}_-$.

Algorithm SM delivers that $\mathcal{F}_{\text{SM}} = \emptyset$, i.e. there are no sliding modes, cf. **Case 3** in Figure 2. If Figure 6 we plot the CPA Lyapunov function computed for the system by solving the LP problem generated by **Algorithm CPA** and in Figure 7 we plot some of its level-sets.

5.2 Example 2

The second example is taken from [18,19], where it was considered as a switched system with state dependent switching between three linear systems. We set $\mathcal{A} := \{1, 2, 3\}$,

$$\mathbf{f}_1(\mathbf{x}) = \begin{pmatrix} -0.1 & 1 \\ -5 & -0.1 \end{pmatrix} \mathbf{x}, \quad \mathbf{f}_2(\mathbf{x}) = \begin{pmatrix} -0.1 & 5 \\ -1 & -0.1 \end{pmatrix} \mathbf{x}, \quad \mathbf{f}_3(\mathbf{x}) = \begin{pmatrix} 1.9 & 3 \\ -3 & -2.1 \end{pmatrix} \mathbf{x},$$

and $\mathcal{D}(\mathbf{f}_i) := \{\mathbf{x} \in \mathbb{R}^2 \,:\, \mathbf{x}^\top Q_i \mathbf{x} \geq 0\}$ with the symmetric matrices

$$Q_1 := \begin{pmatrix} -\frac{1}{1+\sqrt{2}} & -\frac{\sqrt{2}}{2} \\ -\frac{\sqrt{2}}{2} & -1 \end{pmatrix}, \quad Q_2 := \begin{pmatrix} -\frac{2+\sqrt{2}}{2} & -\frac{2+\sqrt{2}}{2} \\ -\frac{2+\sqrt{2}}{2} & -1 \end{pmatrix}, \quad Q_3 := \begin{pmatrix} 1 & \sqrt{2} \\ \sqrt{2} & 1 \end{pmatrix}.$$

It is not difficult to see that the lines

$$y = -(1 + \sqrt{2})x, \quad y = -x, \quad \text{and} \quad y = -(1 + \sqrt{2})^{-1} x$$

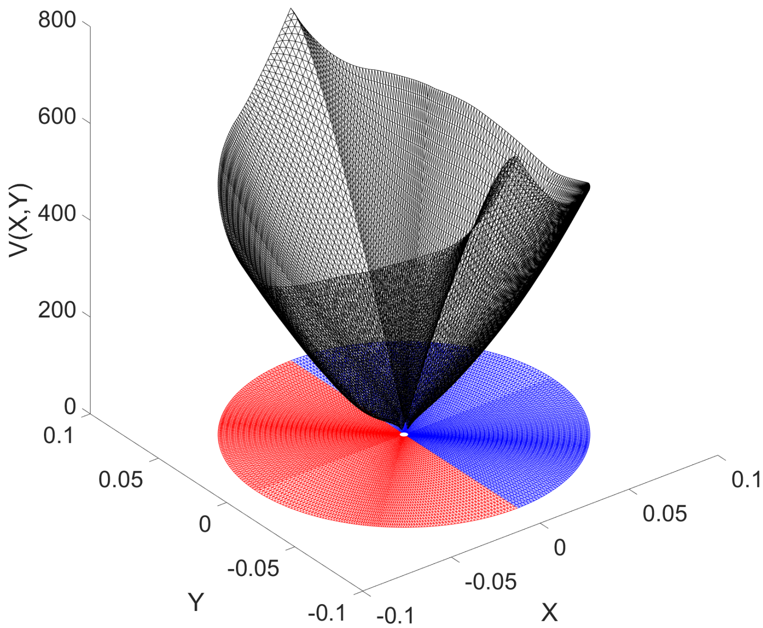

Fig. 6. CPA Lyapunov function computed for (5) (Artstein's circles). The triangles of the domain of $\mathcal{D}(\mathbf{f}_-)$ used in the computations are plotted in red and the triangles of the domain of $\mathcal{D}(\mathbf{f}_+)$ in blue. Note that the Lyapunov function is not defined in a small area of the origin.

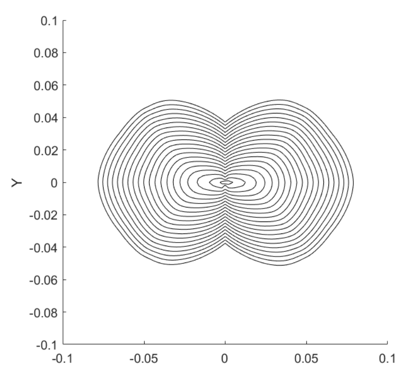

Fig. 7. Level sets of the CPA Lyapunov function from Figure 6 for the system (5) (Artstein's circles). Each level is the boundary of a forward invariant set.

separate the domains $\mathcal{D}(\mathbf{f}_i)$, $i = 1, 2, 3$. To get appropriate areas in our triangulation we first use a triangle fan $\mathcal{T}^{\text{std}}_{N,K}$ with $N = K$ and then map it to match the areas $\mathcal{D}(\mathbf{f}_i)$, $i = 1, 2, 3$. For our discussion it is enough to consider the triangulation in the sector '$x \geq 0$ and $0 \leq y \leq x$', because the triangulation in the sector '$x \geq 0$ and $0 \leq x \leq y$' is obtained by reflection through $y = x$, the sector '$x \leq 0$ and $y \geq 0$' by subsequent reflection through $x = 0$ and the half-plane $y \leq 0$ finally by reflection through $y = 0$.

In the sector '$x \geq 0$ and $0 \leq y \leq x$' the triangle fan consists of triangles with vertices $(0, 0)$, (K, b), and $(K, b + 1)$, where $K > 0$ is a fixed integer and $b = 0, 1, \dots, K-1$. To obtain a triangulation, such that the line segment between $(0, 0)$ and $(K, (1 + \sqrt{2})^{-1}K)$ is the common side of two triangles, we let K be divisible by 5 and define $a = (1 + \sqrt{2})^{-1}$ and map our triangles with $\mathbf{M}(x, y) = \alpha \cdot (x, g(y))^\top$, where $\alpha > 0$ is a scaling factor and

$$g(y) = \begin{cases} \dfrac{a}{0.4} y, & \text{if } 0 \leq y \leq 0.4x \\ ax + (y - 0.4x)\dfrac{1 - a}{1 - 0.4}, & \text{if } 0.4x \leq y \leq x \end{cases}$$

Since K is divisible by 5 the triangles with vertex $(K, 2K/5)$ in the triangulation are mapped to a triangle with the vertex $(K, (1 + \sqrt{2})^{-1}K)$. Reflection through $y = x$ gives triangles with vertex $((1+\sqrt{2})^{-1}K, K)$ and the line segment between this point and the origin is on the line $y = (1 + \sqrt{2})x$. Finally, the reflections through $x = 0$ and $y = 0$ give triangles with $(-K, (1 + \sqrt{2})^{-1}K)$ and $(K, -(1 + \sqrt{2})^{-1}K)$ as vertices, corresponding to the line $y = -(1+\sqrt{2})^{-1}x$, and triangles with $(-(1 + \sqrt{2})^{-1}K, K)$ and $((1 + \sqrt{2})^{-1}K, -K)$ as vertices, corresponding to the line $y = -(1 + \sqrt{2})x$.

In our computations we can set $B^a_{C,r,s} = 0$ uniformly; and we fix $K = 10$ and $\alpha = 5 \cdot 10^{-2}$, see Figure 8 for a graphical representation of the triangulation.

Algorithm SM delivers that $\mathcal{F}_{\text{SM}} = \emptyset$, i.e. there are no sliding modes. The LP problem generated by **Algorithm CPA** was solved in 30 ms and delivers a CPA Lyapunov function on the domain $[-0.5, 0.5]^2$. Since all subsystems are linear this Lyapunov function can be extended radially the the entire plane $\mathbb{R}^2$ with

$$V(\mathbf{x}) = 2\|\mathbf{x}\|_\infty V\left(\frac{\mathbf{x}}{2\|\mathbf{x}\|_\infty}\right) \quad \text{for} \quad \|\mathbf{x}\|_\infty \geq \frac{1}{2}.$$

The computed CPA Lyapunov function is depicted in Figure 9 and some of its level sets in Figure 10.

5.3 Example 3

The third and last example is a nonlinear system from [19]. We set $\mathcal{A} := \{1, 2\}$ and

$$\mathbf{f}_1(\mathbf{x}) = \begin{pmatrix} -0.1 & 1 \\ -5 & -0.1 \end{pmatrix} \mathbf{x} - \begin{pmatrix} \arctan(x_1) \\ \arctan(x_2) \end{pmatrix}, \ \mathbf{f}_2(\mathbf{x}) = \begin{pmatrix} -0.1 & -5 \\ 1 & -0.1 \end{pmatrix} \mathbf{x} - \begin{pmatrix} \arctan(x_1) \\ \arctan(x_2) \end{pmatrix}$$

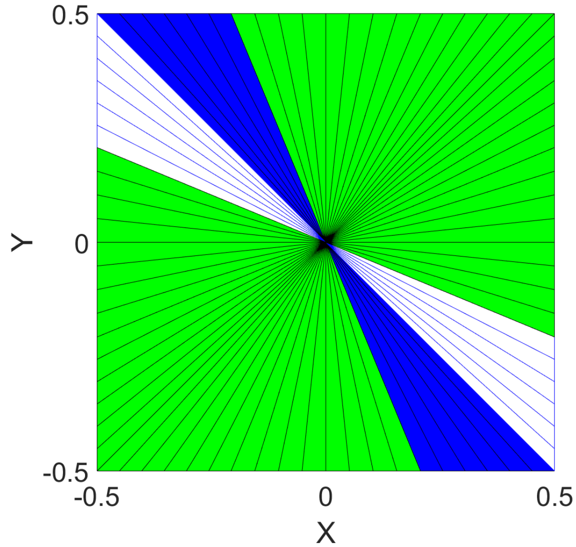

Fig. 8. The triangulation used for the system in Example 5.2. The blue triangles are the triangulation of $\mathcal{D}(\mathbf{f}_1)$, the white triangles the triangulation of $\mathcal{D}(\mathbf{f}_2)$, and the green triangles the triangulation of $\mathcal{D}(\mathbf{f}_3)$.

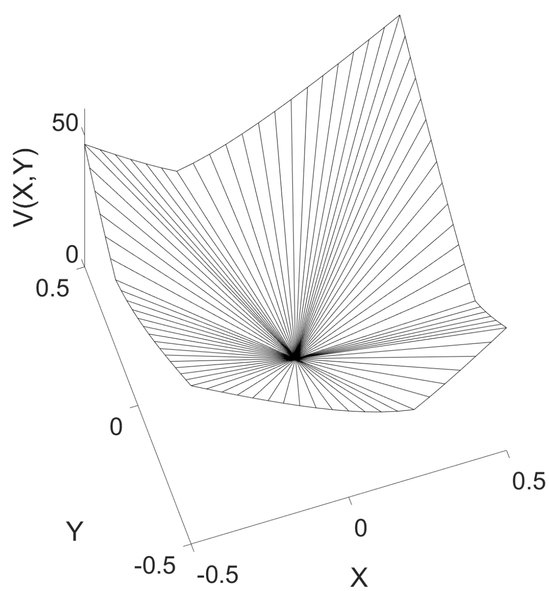

Fig. 9. CPA Lyapunov function computed for the system in Example 5.2. This Lyapunov function can be extended radially to the entire plane $\mathbb{R}^2$.

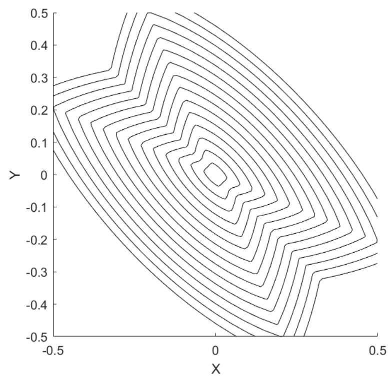

Fig. 10. Level sets of the CPA Lyapunov function computed for the system in Example 5.2, cf. Figure 9. Each level is the boundary of a forward invariant set.

$\mathcal{D}(\mathbf{f}_1) := \{\mathbf{x} \in \mathbb{R}^2 \,:\, x_1^2 - x_2^2 \leq 0\}$ and $\mathcal{D}(\mathbf{f}_2) := \{\mathbf{x} \in \mathbb{R}^2 \,:\, x_1^2 - x_2^2 \geq 0\}$. Hence, the lines $y = x$ and $y = -x$ separate the domains.

We used the mapped standard triangulation $\mathcal{T}_{12,3}^{\text{std}}$ using the mapping $\mathbf{M}(\mathbf{0}) = \mathbf{0}$ and

$$\mathbf{M}(\mathbf{x}) = 5 \cdot 10^{-3} \frac{\|\mathbf{x}\|_\infty^2}{\|\mathbf{x}\|_2} \mathbf{x} \quad \text{for } \mathbf{x} \neq \mathbf{0}.$$

We set as upper bounds $B_{C,r,s}^a = 2 \max_{\mathbf{x} \in C} \|\mathbf{x}\|_\infty$ for all simplices and faces $\operatorname{co} C$.

In this example **Algorithm SM** delivers that $\mathcal{F}_{\text{SM}}$ consists of all faces of simplices on the line $y = x$ except $\{(0,0)\}$, i.e. all sides and all vertices! Note that the vertices on the line are 0-faces of the triangles adjoining the triangles with sides on the line and they must also be considered in **Algorithm CPA**. The faces on the line $y = x$, are repelling, i.e. boundaries of type Case 2 in Figure 2, except for the face $\{\mathbf{0}\}$.

The LP problem generated by **Algorithm CPA** was solved in 0.85 s and delivers a CPA Lyapunov function on a circular disk with radius 0.72. The computed CPA Lyapunov function is depicted in Figure 11 and some of its level sets in Figure 12.

6 CONCLUSIONS

We presented two novel algorithms, **Algorithm SM** and **Algorithm CPA**, for the differential inclusions as defined in Section 3.2. **Algorithm SM** computes a (tight) superset of the sliding modes of the system by verifying certain linear constraints. **Algorithm CPA** uses linear programming to parameterize a continuous and piecewise affine (CPA) Lyapunov function for the system, using information on the location of the sliding modes from **Algorithm SM**. Together they represent a major improvement to the algorithms developed in [31,8,9,10,35] for switched systems and differential inclusions. We show the efficacy of our algorithms by computing the sliding modes and CPA Lyapunov functions for three systems from the literature.

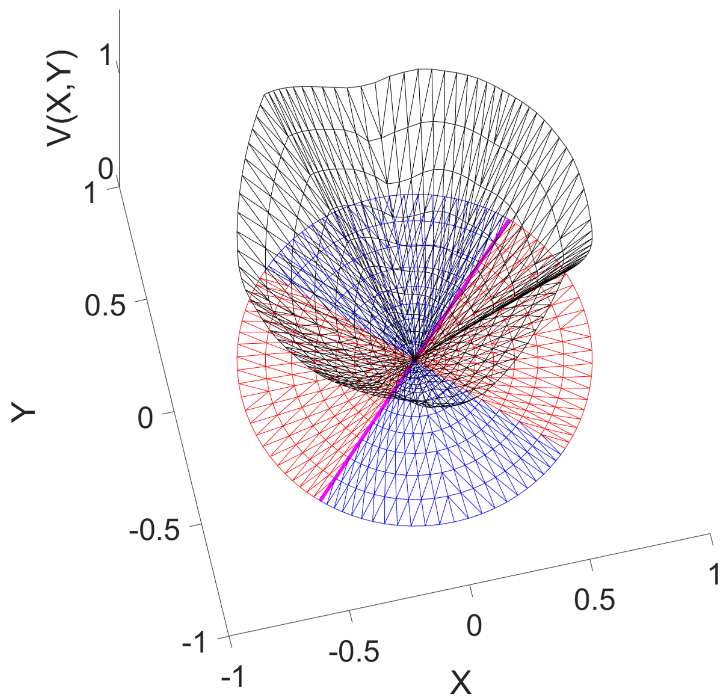

Fig. 11. CPA Lyapunov function computed for the system in Example 5.3.

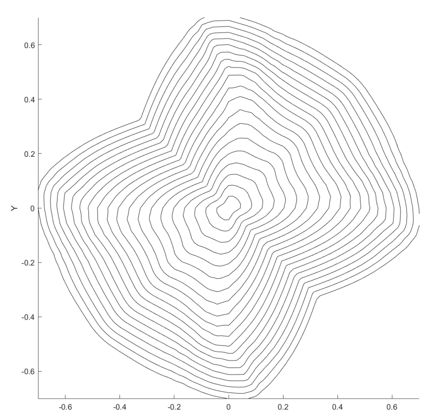

Fig. 12. Level sets of the CPA Lyapunov function from Figure 11 for the system in Example 5.3. Each contour is the boundary of a forward invariant set. Notice the non-convex shape at the repelling line $y = -x$.

References

1. A. Agrachev and D. Liberzon. Lie-algebraic stability criteria for switched systems. *SIAM J. Control Optim.*, 40(1):253–269, 2001.
2. A. Ahmadi and R. Jungers. On complexity of Lyapunov functions for switched linear systems. In *Proceedings of the 19th World Congress of the International Federation of Automatic Control*, volume 47, pages 5992–5997, Cape Town, South Africa, 2014.
3. S. Albertsson, P. Giesl, S. Gudmundsson, and S. Hafstein. Simplicial complex with approximate rotational symmetry: A general class of simplicial complexes. *J. Comput. Appl. Math.*, 363:413–425, 2020.
4. Z. Artstein. Stabilization with relaxed controls. *Nonlinear Anal. Theory Methods Appl.*, 7(11):1163–1173, 1983.
5. J.-P. Aubin and A. Cellina. *Differential Inclusions.* Springer, 1984.
6. J.-P. Aubin and H. Frankowska. *Set-Valued Analysis.* Birkhäuser, 1990.
7. R. Baier, P. Braun, L. Grüne, and C. Kellett. *Large-Scale and Distributed Optimization*, chapter Numerical Construction of Nonsmooth Control Lyapunov Functions, pages 343–373. Number 2227 in Lecture Notes in Mathematics. Springer, 2018.
8. R. Baier, L. Grüne, and S. Hafstein. Computing Lyapunov functions for strongly asymptotically stable differential inclusions. In *IFAC Proceedings Volumes: Proceedings of the 8th IFAC Symposium on Nonlinear Control Systems (NOLCOS)*, volume 43, pages 1098–1103, 2010.
9. R. Baier, L. Grüne, and S. Hafstein. Linear programming based Lyapunov function computation for differential inclusions. *Discrete Contin. Dyn. Syst. Ser. B*, 17(1):33–56, 2012.
10. R. Baier and S. Hafstein. Numerical computation of Control Lyapunov Functions in the sense of generalized gradients. In *Proceedings of the 21st International Symposium on Mathematical Theory of Networks and Systems (MTNS)*, pages 1173–1180 (no. 0232), Groningen, The Netherlands, 2014.
11. F. Bakhshande, R. Bach, and D. Söffker. Robust control of a hydraulic cylinder using an observer-based sliding mode control: Theoretical development and experimental validation. *Control Eng. Pract.*, 95:no. 104272, 2020.
12. J. Björnsson, Gudmundsson, and S. Hafstein. Class library in C++ to compute Lyapunov functions for nonlinear systems. In *Proceedings of MICNON, 1st Conference on Modelling, Identification and Control of Nonlinear Systems*, pages 788–793 (no. 0155), 2015.
13. M. Branicky. Multiple Lyapunov functions and other analysis tools for switched and hybrid systems. *IEEE Trans*, 43(4):475–482, 1998.
14. F. Clarke. *Optimization and Nonsmooth Analysis.* Classics in Applied Mathematics. SIAM, 1990.
15. F. Clarke, Y. Ledyaev, and R. Stern. Asymptotic stability and smooth Lyapunov functions. *J. Differential Equations*, 149:69–114, 1998.
16. G. Davrazos and N. Koussoulas. A review of stability results for switched and hybrid systems. In *Proceedings of 9th Mediterranean Conference on Control and Automation*, Dubrovnik, Croatia, 2001.
17. K. Deimling. *Multivalued Differential Equations.* Walter de Gruyter, 1992.
18. M. Della Rossa, A. Tanwani, and L. Zaccarian. Max-Min Lyapunov functions for switching differential inclusions. In *Proceedings of the 57th IEEE Conference on Decision and Control*, pages 5664–5669, 2018.

19. M. Della Rossa, A. Tanwani, and L. Zaccarian. Max-min Lyapunov functions for switched systems and related differential inclusions. *Automatica*, 120:Article 109123, 2020.
20. C. Edwards and S. Spurgeon. *Sliding Mode Control: Theory And Applications*. Taylor & Francis, 1 edition, 1998.
21. A. Filippov. *Differential Equations with Discontinuous Right-hand Side*. Kluwer, 1988. Translated from Russian, original book from 1985.
22. P. Giesl and S. Hafstein. Existence of piecewise affine Lyapunov functions in two dimensions. *J. Math. Anal. Appl.*, 371(1):233–248, 2010.
23. P. Giesl and S. Hafstein. Existence of piecewise linear Lyapunov functions in arbitrary dimensions. *Discrete Contin. Dyn. Syst. Ser. A*, 32(10):3539–3565, 2012.
24. P. Giesl and S. Hafstein. Computation of Lyapunov functions for nonlinear discrete time systems by linear programming. *J. Difference Equ. Appl.*, 20(4):610–640, 2014.
25. P. Giesl and S. Hafstein. Implementation of a fan-like triangulation for the CPA method to compute Lyapunov functions. In *Proceedings of the 2014 American Control Conference*, pages 2989–2994 (no. 0202), Portland (OR), USA, 2014.
26. P. Giesl and S. Hafstein. Revised CPA method to compute Lyapunov functions for nonlinear systems. *J. Math. Anal. Appl.*, 410:292–306, 2014.
27. P. Giesl and S. Hafstein. System specific triangulations for the construction of CPA Lyapunov functions. *Discrete Contin. Dyn. Syst Ser. B*, to be published, 2021.
28. R. Goebel, A. Teel, T. Hu, and Z. Lin. Conjugate convex Lyapunov functions for dual linear differential inclusions. *IEEE Trans. Automat. Control*, 51(4):661–666, 2006.
29. S. Hafstein. A constructive converse Lyapunov theorem on exponential stability. *Discrete Contin. Dyn. Syst. Ser. A*, 10(3):657–678, 2004.
30. S. Hafstein. A constructive converse Lyapunov theorem on asymptotic stability for nonlinear autonomous ordinary differential equations. *Dynamical Systems: An International Journal*, 20(3):281–299, 2005.
31. S. Hafstein. *An algorithm for constructing Lyapunov functions*, volume 8 of *Monograph*. Electron. J. Diff. Eqns. (monograph series), 2007.
32. S. Hafstein. Implementation of simplicial complexes for CPA functions in C++11 using the armadillo linear algebra library. In *Proceedings of the 3rd International Conference on Simulation and Modeling Methodologies, Technologies and Applications (SIMULTECH)*, pages 49–57, Reykjavik, Iceland, 2013.
33. S. Hafstein. Efficient algorithms for simplicial complexes used in the computation of Lyapunov functions for nonlinear systems. In *Proceedings of the 7th International Conference on Simulation and Modeling Methodologies, Technologies and Applications (SIMULTECH)*, pages 398–409, 2017.
34. S. Hafstein. *Simulation and Modeling Methodologies, Technologies and Applications*, volume 873 of *Advances in Intelligent Systems and Computing*, chapter Fast Algorithms for Computing Continuous Piecewise Affine Lyapunov Functions, pages 274–299. Springer, 2019.
35. S. Hafstein. CPA Lyapunov functions: Switched systems vs. differential inclusions. In *Proceedings of the 17th International Conference on Informatics in Control, Automation and Robotics (ICINCO)*, pages 745–753, 2020.
36. S. Hafstein, C. Kellett, and H. Li. Computing continuous and piecewise affine Lyapunov functions for nonlinear systems. *Journal of Computational Dynamics*, 2(2):227 – 246, 2015.

37. S. Hafstein and H. Li. Computation of Lyapunov functions for nonautonomous systems on finite time-intervals by linear programming. *J. Math. Anal. Appl.*, 447(2):933–950, 2017.
38. H. Li, R. Baier, L. Grüne, S. Hafstein, and F. Wirth. Computation of local ISS Lyapunov functions via linear programming. In *Proceedings of the 21st International Symposium on Mathematical Theory of Networks and Systems (MTNS)*, pages 1189–1195 (no. 0158), Groningen, The Netherlands, 2014.
39. H. Li, S. Hafstein, and C. Kellett. Computation of continuous and piecewise affine Lyapunov functions for discrete-time systems. *J. Difference Equ. Appl.*, 21(6):486–511, 2015.
40. D. Liberzon. *Switching in systems and control*. Systems & Control: Foundations & Applications. Birkhäuser, 2003.
41. S. Marinósson. Lyapunov function construction for ordinary differential equations with linear programming. *Dynamical Systems: An International Journal*, 17:137–150, 2002.
42. S. Marinósson. *Stability Analysis of Nonlinear Systems with Linear Programming: A Lyapunov Functions Based Approach*. PhD thesis: Gerhard-Mercator-University Duisburg, Duisburg, Germany, 2002.
43. A. Molchanov and E. Pyatnitskiĭ. Criteria of asymptotic stability of differential and difference inclusions encountered in control theory. *Systems Control Lett.*, 13(1):59–64, 1989.
44. R. Shorten, F. Wirth, O. Mason, K. Wulff, and C. King. Stability criteria for switched and hybrid systems. *SIAM Review*, 49(4):545–592, 2007.
45. E. Sontag. A Lyapunov-like characterization of asymptotic controllability. *SIAM J. Control Optimization*, 21(3):462–471, 1983.
46. E. Sontag and H. Sussman. Nonsmooth control-Lyapunov functions. In *Proceedings of the 34th IEEE Conference on Decision and Control*, volume 3, pages 2799–2805, New Orleans (LA), USA, 1995.
47. Z. Sun and S. Ge. *Stability Theory of Switched Dynamical Systems*. Communications and Control Engineering. Springer, 2011.
48. W. Walter. *Ordinary Differential Equation*. Springer, 1998.
49. C. Yfoulis and R. Shorten. A numerical technique for the stability analysis of linear switched systems. *Int. J. Control*, 77(11):1019–1039, 2004.
50. K. Young, V. Utkin, and Ü. Özgüner. A control engineer's guide to sliding mode control. *IEEE Trans. Control Syst. Technol.*, 7(3):328–342, 1999.